

Noncontact measurement of transport properties of long-bulk-carrier-lifetime Si wafers using photothermal radiometry

Alex Salnick, Andreas Mandelis, and Claude Jean^{a)}

Department of Mechanical and Industrial Engineering, Photothermal and Optoelectronic Diagnostics Laboratory, University of Toronto, 5 King's College Road, Toronto, Ontario M5S 3G8, Canada

(Received 12 June 1996; accepted for publication 22 August 1996)

A theoretical model for the photothermal radiometric signal from semiconductors of finite thickness has been used to measure simultaneously the carrier diffusion coefficient, carrier lifetime, and surface recombination velocity of FZ Si wafers with very long bulk carrier lifetimes (industrial microelectronic grade). The results showed the importance of accounting for the finite thickness of the substrate in obtaining accurate measurements of these parameters using the entirely noncontacting radiometric approach. © 1996 American Institute of Physics. [S0003-6951(96)02143-2]

Photothermal infrared radiometric (PTR) measurements of photoexcited excess carrier lifetime in a semiconductor using both frequency domain¹⁻³ and rate-window^{4,5} detection configurations have been reported. A semi-infinite semiconductor sample approach assuming the carrier diffusion length much shorter than the sample thickness has been used. However, for long lifetime (>100 μs) and/or thin (<500 μm) semiconductor wafers the foregoing approximation is not valid and the effects introduced by a finite thickness should be taken into account.

In this letter we report a feasibility study of the PTR technique to measure carrier transport parameters in industrially relevant long bulk lifetime FZ-Si wafers.

It has been shown earlier that the photoinjected excess carrier concentration $\Delta N(x)$ [m⁻³] as a solution of the one-dimensional carrier continuity equation for a finite semiconductor of thickness L [m] with optical absorption coefficient α [m⁻¹], minority carrier lifetime τ [s], carrier diffusivity D_n [m²/s] and the front and back surface recombination velocities s_1 and s_2 [m/s], respectively, are

$$\Delta N(x) = \frac{\alpha \eta I_0}{h\nu D(\alpha^2 - \sigma_n^2)} \left(\frac{\gamma_1 \Gamma_2 - \gamma_2 \Gamma_1 e^{-L(\alpha + \sigma_n)}}{\Gamma_2 - \Gamma_1 e^{-2\sigma_n L}} e^{-\sigma_n x} + \frac{\gamma_1 - \gamma_2 e^{-L(\alpha - \sigma_n)}}{\Gamma_2 - \Gamma_1 e^{-2\sigma_n L}} e^{\sigma(x-2L)} - e^{-\alpha x} \right), \quad (1)$$

where

$$S_{PTR} = \frac{\text{const}}{D_n \sigma_n (\alpha^2 - \sigma_n^2)} \left(\frac{(\gamma_1 \Gamma_2 - x_2 \Gamma_1 e^{-L(\alpha + \sigma_n)} + \gamma_1 e^{-\sigma_n L} - \gamma_2 e^{-\alpha L})(1 - e^{-\sigma_n L})}{\Gamma_2 - \Gamma_1 e^{-2\sigma_n L}} - \frac{\sigma_n}{\alpha} (1 - e^{-\alpha L}) \right). \quad (5)$$

Assuming a strong optical absorption at the front surface $\alpha L \gg 1$ and, in addition, $\alpha \gg |\sigma_n|$, Eq. (5) reduces to

$$S_{PTR} = \text{const} \left[\frac{1 - e^{-\sigma_n L}}{\sigma_n (D_n \sigma_n + s_1)} \right] \left[\frac{\Gamma_2 + e^{-\sigma_n L}}{\Gamma_2 - \Gamma_1 e^{-2\sigma_n L}} \right] \quad (6)$$

^{a)}MITEL S.C.C. Bromont, Québec J0E 1L0, Canada.

$$\begin{aligned} \Gamma_1 &= \frac{D_n \sigma_n - s_1}{D_n \sigma_n + s_1}, \\ \Gamma_2 &= \frac{D_n \sigma_n + s_2}{D_n \sigma_n - s_2}, \\ \gamma_1 &= \frac{D_n \alpha + s_1}{D_n \sigma_n + s_1}, \\ \gamma_2 &= \frac{D_n \alpha - s_2}{D_n \sigma_n - s_2}, \end{aligned} \quad (2)$$

and I_0 [W cm⁻²] is the light flux, $h\nu$ is the photon energy [J], and the complex plasma-wave vector σ_n is defined as

$$\sigma_n = \sqrt{(1 + i\omega\tau)/D_n\tau}. \quad (3)$$

The PTR signal from a plasma-dominated semiconductor has been shown to be proportional to⁶

$$S_{PTR} \sim \int_0^L \Delta N(x) dx. \quad (4)$$

Upon calculating the foregoing integral for $\Delta N(x)$ from Eq. (1) we obtain

and for rough unpolished back surface ($s_2 \gg D_n |\sigma_n|$) $\Gamma_2 \cong -1$ in Eq. (2) and the PTR signal can be written as

$$S_{PTR} = \frac{\text{const}}{D_n \sigma_n (D_n \sigma_n + s_1)} \left\{ \frac{(1 - e^{-\sigma_n L})^2}{1 + \Gamma_1 e^{-2\sigma_n L}} \right\} \quad (7)$$

or

$$S_{PTR} = S_{PTR}^\infty \left\{ \frac{(1 - e^{-\sigma_n L})^2}{1 + \Gamma_1 e^{-2\sigma_n L}} \right\}, \quad (8)$$

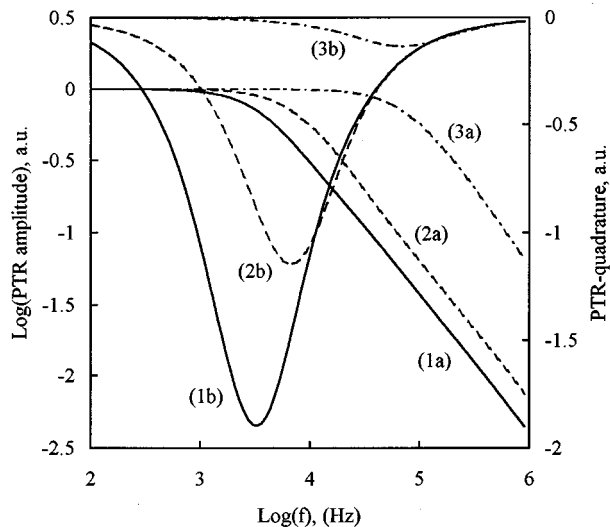


FIG. 1. The PTR-amplitude and PTR-quadrature component (right scale) frequency responses calculated using the theoretical model for finite semiconductors of various thicknesses: $L=1000\ \mu\text{m}$ (1a,b), $500\ \mu\text{m}$ (2a,b), and $100\ \mu\text{m}$ (3a,b). Parameters used for the calculation: $\tau=100\ \mu\text{s}$, $D_n=20\ \text{cm}^2/\text{s}$, $s_1=500\ \text{cm/s}$.

where S_{PTR}^{∞} is the PTR signal from semi-infinite semiconductor⁶ and the term in brackets represents the contribution from assumption of the finite wafer thickness.

The effect of the wafer thickness on the PTR amplitude and quadrature component frequency responses calculated using Eq. (8) is illustrated in Fig. 1.

The quadrature component of the PTR signal was found to be very important and useful parameter in PTR studies of semiconductors. Being close to zero at both low and high frequency limits, it exhibits a sharp clear negative peak at the modulation frequency where $\omega\tau\sim 1$ (Fig. 1), thus allowing for the fast estimation of the lifetime and for more precise fitting to the theoretical model, than has been done⁶ using the PTR phase.

As it has been stated in previous radiometric studies of semi-infinite semiconductors^{1,3,6} the PTR-amplitude frequency response consists of two characteristic regions: the flat plateau at low frequencies ($\omega\tau\ll 1$) and a $\sim\omega^{-1}$ drop at high frequencies ($\omega\tau\gg 1$) with the slope breakpoint at $\omega\tau\sim 1$.

As can be seen from Fig. 1, in the case of a finite wafer, decreasing L shifts the slope breakpoint to higher frequency, so that the entire frequency response looks as if the sample had a shorter lifetime. The same effective lifetime “decrease-equivalent” effect was observed for the frequency responses of the PTR-phase, PTR-in-phase and PTR-quadrature components.

The PTR instrumentation setup used in the present study was described in detail previously.⁵ An Ar^+ laser emitting $\sim 1\ \text{W}$ at $514\ \text{nm}$ was used as an excitation source. The modulation square waveform of the laser-beam intensity was controlled by an acousto-optic modulator. The modulation frequency range used was $100\ \text{Hz}$ – $100\ \text{kHz}$. The laser beam size was $5\ \text{mm}$ to satisfy the one-dimensionality of the PTR signal. The lower limit was chosen so as to prevent the thermal component from dominating the PTR signal. Special arrangements of the set up have been made to fit the large-size wafers (diameter $100\ \text{mm}$).

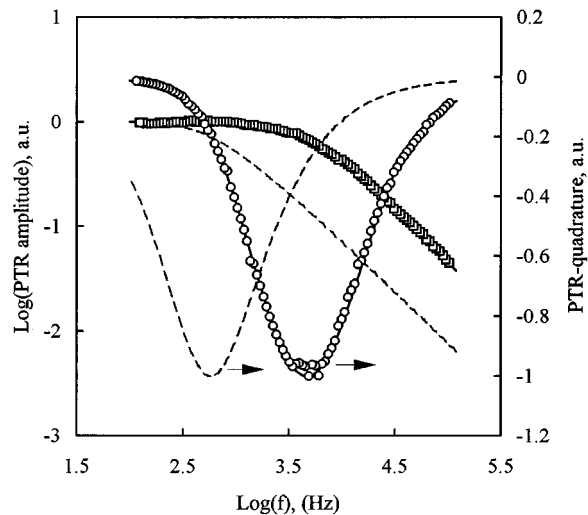


FIG. 2. Experimental PTR-amplitude (\square) and PTR-quadrature component (\circ) frequency responses of p -Si sample obtained at $300\ \text{K}$ and the results of the best fitting (dashed lines) with $D_n=32\ \text{cm}^2/\text{s}$, $s_1=210\ \text{cm/s}$ and $\tau=350\ \mu\text{s}$. Dotted lines represent the frequency responses simulated using the same parameters and the semi-infinite model.

One FZ p -Si wafer (10 – $15\ \Omega\ \text{cm}$, $L=525\ \mu\text{m}$) from MITEL S.C.C. (Bromont, Québec, Canada) was studied. According to the manufacturer’s certificate, it has $\tau>100\ \mu\text{s}$ at room temperature.

Figure 2 represents the experimental PTR-amplitude and PTR-quadrature frequency responses measured at room temperature. Both amplitude and quadrature components follow the theoretical predictions. The high-frequency log–log amplitude slope of -1 indicates a low surface recombination velocity s_1 .^{1,6}

The three-parameter fitting of the foregoing frequency responses by the theoretical model, Eq. (7), resulted in a very good correlation (solid lines in Fig. 2 are overlapped by the experimental points) and yielded the following carrier transport parameters: $\tau=350\ \mu\text{s}$, $s_1=210\ \text{cm/s}$, and $D_n=32\ \text{cm}^2/\text{s}$.

The importance of accounting for the finite thickness of Si wafer is clear from the comparison of experimental data and corresponding fitting curves with responses simulated using the same parameters and a semi-infinite model for the PTR signal S_{PTR}^{∞} , Eq. (8), presented as dotted lines in Fig. 2. It can be shown that the foregoing difference becomes even more significant for longer lifetime and/or thinner wafer.

We wish to gratefully acknowledge the support of the Natural Sciences and Engineering Research Council of Canada (NSERC) for a Collaborative Research Grant. One of us (A.S.) is also grateful to NSERC for a NATO Science Research Fellowship Award.

¹S. J. Sheard, M. G. Somekh, and T. Hiller, Mater. Sci. Eng. B **5**, 101 (1990).

²T. M. Hiller, M. G. Somekh, S. J. Sheard, and D. R. Newcombe, Mater. Sci. Eng. B **5**, 107 (1990).

³S. Sheard and M. Somekh, *Progress in Photothermal and Photoacoustic Science and Technology*, Vol. II: Nondestructive Evaluation (NDE), edited by A. Mandelis (Prentice Hall, Englewood Cliffs, NJ, 1994), pp. 112–150.

⁴A. Mandelis and Z. H. Chen, *Rev. Sci. Instrum.* **63**, 2977 (1992).

⁵Z. H. Chen, R. Bleiss, A. Mandelis, A. Buczkowski, and F. Shimura, *J. Appl. Phys.* **73**, 5043 (1993).

⁶A. Salnick, C. Jean, and A. Mandelis (unpublished).

⁷A. Mandelis, R. A. Budiman, M. Vargas, and D. Wolff, *Appl. Phys. Lett.* **67**, 1582 (1995).